PROCEEDINGS OF SCIENCE

Preparing for LHC data-taking with the ATLAS experiment

Fabiola Gianotti[*†]
CERN
E-mail: fabiola.gianotti@cern.ch

The status of the ATLAS experiment a few months before the start-up of LHC operation is described. Emphasis is given to the preparation for the imminent data-taking phase through commissioning studies with cosmics data. A few examples of the physics potential and goals with early LHC data are also presented.

The 2009 Europhysics Conference on High Energy Physics,
July 16 - 22 2009
Krakow, Poland

[*]Speaker.
[†]Representing the ATLAS Collaboration.

PoS(EPS-HEP 2009)005

1. Introduction

The history of the ATLAS experiment started a long time ago, in the early '90s, with vigorous R&D activities to develop detector techniques suitable for operation in the harsh environment of the CERN Large Hadron Collider (LHC, [1]), and first ideas for the detector's design. The experiment was approved in 1996, construction started one year later, and installation in the underground cavern took place between 2003 and 2008. It has been followed by an intense commissioning phase based on cosmics data recorded with the full detector operational in its final position. Finally, in September 2008 ATLAS successfully collected LHC single-beam data.

The ATLAS history covers also 20 years of test-beam activities and simulation studies of the detector performance and physics potential, eight years of worldwide computing " data challenges", 17 Technical Design Reports submitted to review committees, and a rich education and outreach programme. These achievements are the results of huge efforts of a worlwide Collaboration, which consists of almost 3000 scientists from 169 Institutions and 37 countries.

In July 2009, at the time of the EPS-HEP 2009 Conference, ATLAS was in its final preparation phase for first LHC collisions, expected to happen in Fall 2009. This paper presents the status of the experiment at that time, as well as the physics prospects with first LHC data. Section 2 describes the ATLAS detector and the status of the experiment at the time of the Conference, while section 3 discusses the detector commissioning with cosmics and single-beam data. Section 4 presents examples of the expected physics potential with early LHC data, and section 5 is devoted to the conclusions.

2. Status of the experiment

A schematic view of the ATLAS detector [2] is shown in figure 1. It is about 46 m long and 25 m high, it weighs about 7000 tons, and the signals produced by the collision products are read out by about 100 million independent electronic channels.

The tracking devices surrounding the beam pipe consist of layers (in the barrel part) and disks (in the end-caps) of Pixels and Silicon strips (Semiconductor tracker, SCT), followed by a Transition radiation detector (made of straw-tube type drift chambers filled with $Xe/CO_2/O_2$ gas). This whole system, which provides precise tracking and vertexing with a momentum resolution of better than 4% up to $\sim$100 GeV, is immersed in a 2 Tesla (T) field produced by a superconducting solenoid located in front of the electromagnetic calorimeter.

The electromagnetic calorimeter is a lead-liquid argon sampling detector with accordion shape, fine granularity for powerful electron and photon identification, and energy resolution of about $\sim$ $10\%/\sqrt{E\,(\mathrm{GeV})}$.

The hadron calorimetry includes an iron-scintillating tiles calorimeter (Tile) in the central part, and liquid-argon detectors with copper and tungsten absorbers in the forward regions (where the radiation levels are higher). This system provides excellent hermeticity over the full azimuthal angle and rapidity range $|\eta| < 5$, as well as good granularity ($\Delta\eta \times \Delta\phi \sim 0.1 \times 0.1$), for precise measurements of jets and of the event missing transverse energy. The hadronic energy resolution is about $50\%/\sqrt{E\,(\mathrm{GeV})}$.

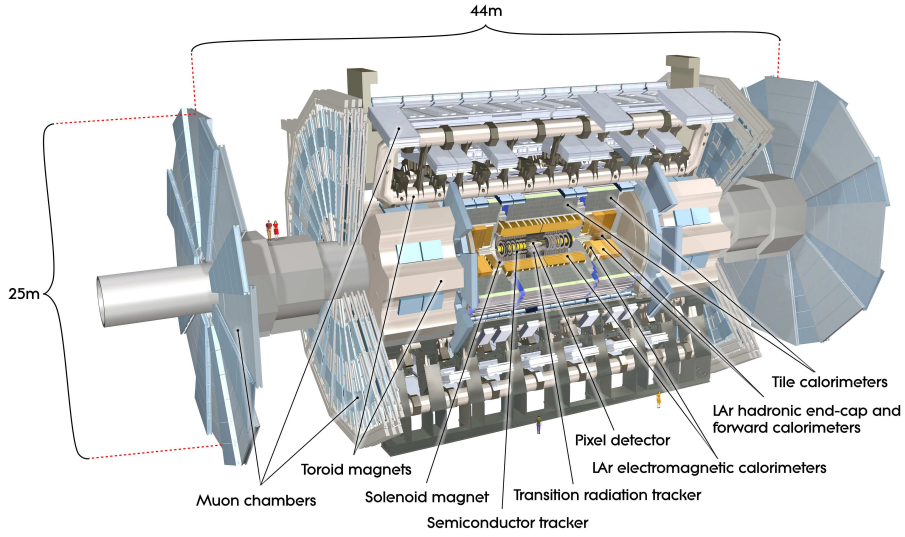

Figure 1: Layout of the ATLAS detector.

Finally, the external muon spectrometer, which extends over an area corresponding to three football fields, consists of gas-based chambers in air, immersed in strong toroidal magnetic fields (up to $\sim$9 Tm). In the central region, the field is provided by eight giant superconducting coils (about 25 m long, $\sim$100 ton each), and in the forward regions by two end-cap toroid magnets. This magnet system, which works at a temperature of 4.5 K, has been operated at full current (20 kA for the toroids, 7.7 kA for the solenoid) over extended periods. The barrel muon chambers are arranged in three radial stations, and include Monitoring Drift Tubes (MDT) for precision measurements and Resistive Plate Chambers (RPC) for trigger purposes. The end-cap chambers are installed in small and big wheels, six wheels at each side of the collision centre. MDT and Cathode Strip Chambers (CSC) technologies are used for precision measurements, whereas the trigger is based on Thin Gap Chambers (TGC). The muon spectrometer provides efficient muon trigger, identification and measurements, with a momentum resolution of better than 10% up to $\sim$1 TeV.

A three-level trigger system selects about 200 Hz of interesting events for recording to mass storage, out of 40 MHz (at the LHC design operation) of beam-beam collisions. It is based on programmable hardware devices at level-one, which use the fast signals from the calorimeters and the muon spectrometer, and on sophisticated software algorithms running on a farm of $\sim$1000 PC boxes at the higher levels.

Spectacular views of some detector components are presented in figures 2– 4. Figure 2 shows the ATLAS cavern in October 2005, with the full barrel toroid magnet system in place and the barrel calorimeter (liquid-argon electromagnetic and Tile hadronic) in its final position at Z=0 (corresponding to the nominal beam-beam interaction centre).

The innermost ATLAS device, the Pixel detector, is shown in figure 3. This high-technology instrument consists of 80 million 50×400 μm^2 size pixels, carried by 1744 modules arranged in three barrel layers (the innermost one sitting at 5 cm from the beam line) and six end-cap disks (three at each side of the collision centre). Such a high readout granularity is needed to cope with the high track density expected in the region surrounding the beam pipe when the LHC operates

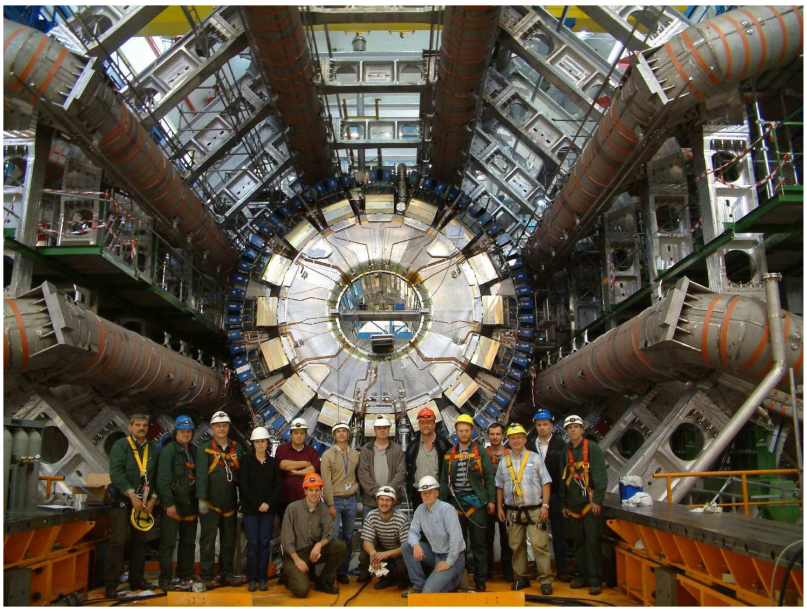

Figure 2: The ATLAS barrel calorimeter in its final position inside the barrel toroid system in October 2005. The cryostat housing the liquid-argon electromagnetic calorimeter and the solenoid is surrounded by the hadronic Tile calorimeter.

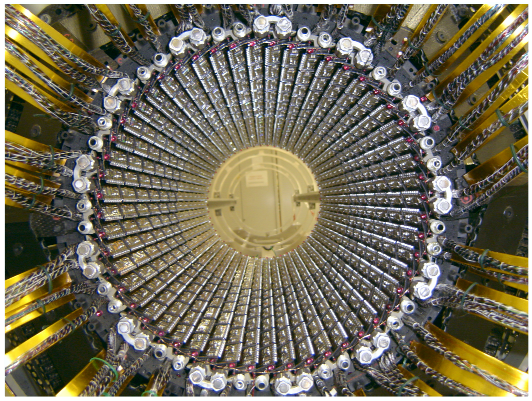

Figure 3: The outermost layer of the barrel pixel detector.

close to design luminosity.

Finally, figure 4 shows a picture of one of the TGC forward wheels. It has a radius of about 12.5 m.

Over the last years, cosmic-ray data have been collected over extended periods for commissioning purposes. More than 600 million events have been recorded in 2008 and 2009 with the full detector operational, and many more with individual (or group of) detectors in the previous years.

In September 2008, when first (single) beams started to circulate in the LHC, ATLAS recorded samples of single-beam data. These data have been very useful to commission the detector in a complementary way to the cosmics data, e.g. for timing studies (see section 3). Following the

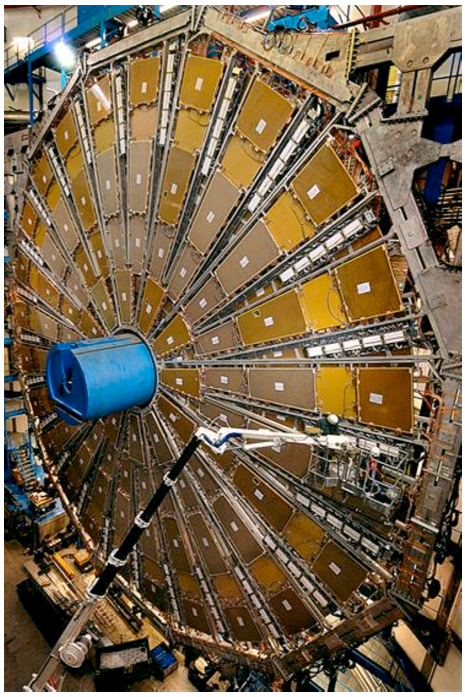

Figure 4: One of the forward wheels of the ATLAS muon spectrometer, carrying the TGC muon trigger chambers.

Detector system	Total number of channels	Approximate operational fraction (%)
Pixels	80 million	98.5
Silicon strips (SCT)	6.3 million	99.5
Transition Radiation detector (TRT)	350000	98.2
Liquid-argon electromagnetic calorimeter	170000	99.5
Tile hadronic calorimeter	9800	99.5
Liquid-argon hadronic end-cap calorimeter	5600	99.9
Liquid-argon forward calorimeter	3500	100
Muon Drift Tube chambers (MDT)	350000	99.3
Muon Cathode Strip chambers (CSC)	31000	98.5
Muon barrel trigger chambers (RPC)	370000	95.5
Muon end-cap trigger chambers (TGC)	320000	99.5

Table 1: For the various ATLAS detector components, the total numbers of readout channels, and the approximate fractions of operating channels as of July 2009.

LHC incident a few days later (19 September 2009, [3]), the detector was opened for some repairs and consolidation work. It was closed again at the beginning of June 2009, and cosmics data-taking has resumed since then.

The status of the detector at the time of the conference is summarized in table 1. The fractions of non-operating channels are at the level of a few per mil in most cases, which is a remarkable achievement for a detector of this complexity.

Another challenging component of the LHC experiments is the computing infrastructure and

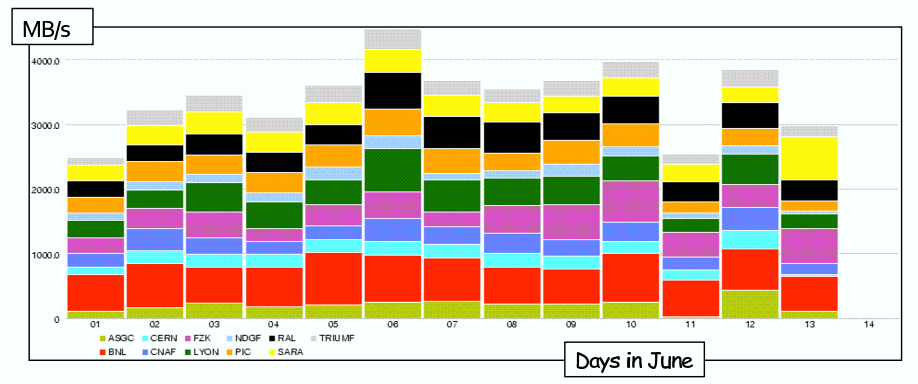

Figure 5: Data-transfer rate among ATLAS centres (Tier-0→Tier-1s and Tier-1s→Tier1-s) achieved in June 2009, using a mixture of cosmic-ray data and simulation samples. The colours indicate the various centres.

operation. The ATLAS worldwide computing system, based on the wLCG grid [4], consists of about 70 sites, organized in a hierarchical structure ("tiers"). It includes the CERN computing centre (so-called Tier-0), ten big regional centres (called Tier-1), and several smaller sites (Tier-2 federations). During LHC data-taking, ATLAS will have to distribute more than 50 Petabytes (PB) of data all over the globe, to allow the worldwide collaboration to do physics analysis in an effective way. Furthermore, 1 billion events from the detector will have to be reconstructed and reprocessed every year, not including simulation samples. These and other challenging operations have been exercised and stress-tested over the last years through functional tests and "data challenges" of increasing functionality, size and realism. An example is shown in figure 5: in June 2009, during a dedicated data challenge, data-transfer rates from CERN to Tier-1s and among Tier-1s of up to 4 GB/s have been achieved (and sustained over a period of two weeks), which is twice as large as the nominal throughput expected during LHC operation.

3. Detector commissioning with cosmics and single-beam data

Cosmic rays have provided the first source of real data to commission the full detector *in situ*. These data have proved to be very useful to find and fix problems (e.g. cabling mistakes), to perform first calibration and alignment studies, and to gain global operation experience. A few examples (out of a huge amount) of results are discussed below.

Figure 6 shows a cosmic muon traversing ATLAS from top to bottom and leaving signals in the various sub-detectors.

The trigger system is a crucial component of an experiment at a hadron collider, and has to be ready to work efficiently as soon as collisions become available. Figure 7 shows the nice correlation between the energy measured by the hardware-based level-one calorimeter trigger, which has a coarse granularity, and the energy measured by the more granular and precise calorimeter readout electronics.

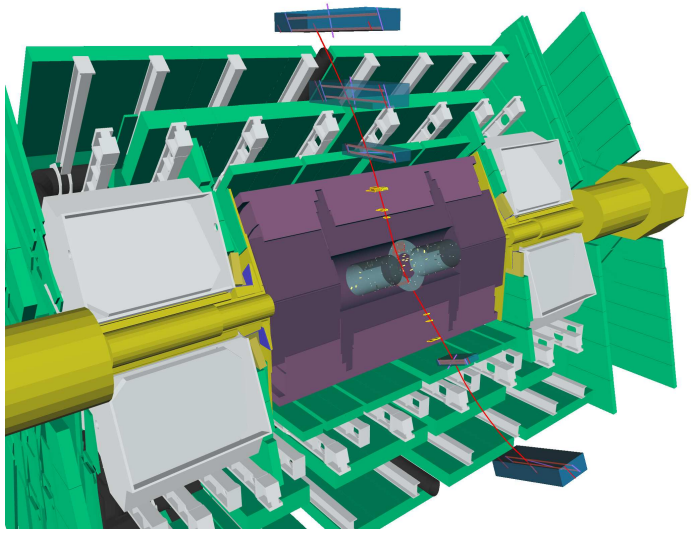

Figure 6: A cosmic-ray muon event recorded on 18 October 2008.

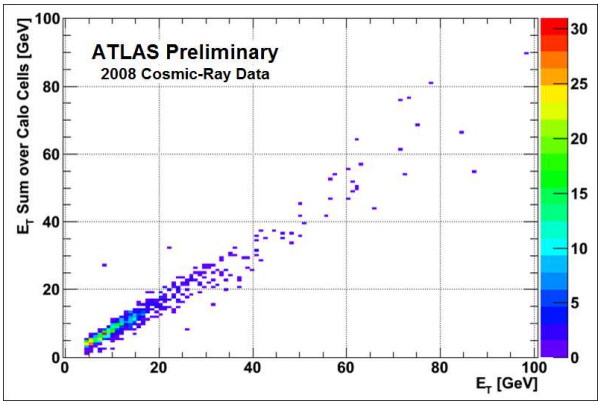

Figure 7: Cosmic-muon shower energy measured with the calorimeter readout electronics, as a function of the energy measured in coarser trigger towers by the level-one calorimeter trigger. Initial calibration constants have been used (more refined calibrations are expected to reduce the energy spread).

The more sophisticated higher-level triggers (level two and level three) have also been run routinely, even if they are not needed to select (the simple) cosmics events: more than 150 high-level trigger chains have been extensively tested during cosmics data-taking.

Figure 8 shows examples of correlations between measurements made by two different systems (inner detector and muon spectrometer) for the muon direction (left panel) and muon momentum (right panel). The distribution of the difference between the muon momentum measured by the inner detector and the muon spectrometer, which is well reproduced by the simulation, does not peak at zero. The reason is that only muons in the bottom part of the detector are included in the figure, for which the momentum in the muon spectrometer is smaller than in the inner detector because muons lose on average $\sim$3 GeV in traversing the calorimeters. These results demonstrate the successful operation of several detector systems together, and that the overall performance is well understood.

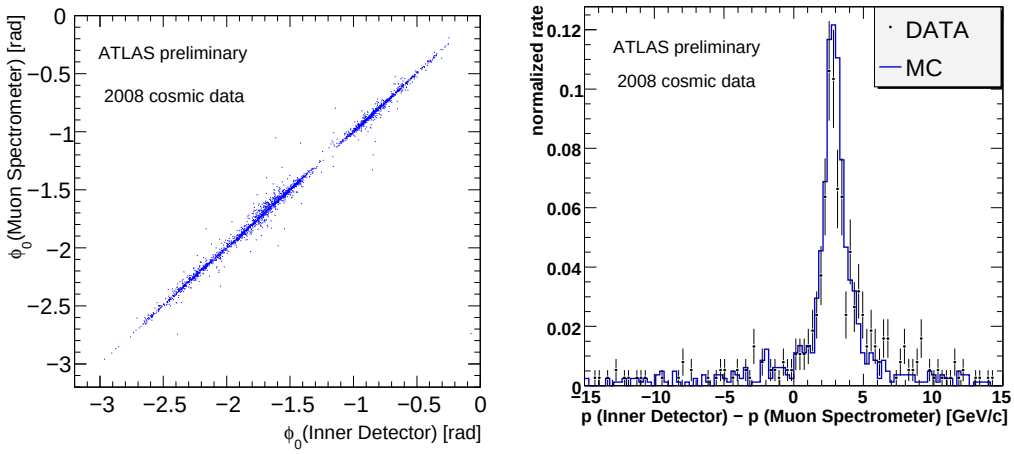

Figure 8: Left: The muon angle with respect to the vertical direction, as measured in the muon spectrometer, as a function of the measurement from the inner detector. Right: The difference between the muon momentum measured by the two systems for the data (dots) and the Monte Carlo simulation of the cosmics set-up (full blue line). Data and Monte Carlo are normalised to the same number of events.

Not only general sanity checks, but also several precision studies have been made with cosmics data, and accuracies have been achieved that in some cases go beyond the expectations at these early stages of the experiment. As an example, figure 9 shows the distributions of the Pixel residuals before and after aligning the detector using cosmic-ray data. The residuals are defined as the distances between the fitted tracks and the hits in the individual layers of the Pixel detector. The widths of the distributions before and after alignment demonstrate how useful cosmics events have been to improve the precise knowledge of the detector. A comparison with the Monte Carlo distribution, which was obtained with a perfectly aligned geometry, indicates that the remaining misalignment in the data is at the level of ~ 20 μm (to be compared with the ultimate goal of 5–10 μm needed for LHC precision physics). The stability of the alignment constants with time was also measured over several months, and was found to be at the level of a few microns.

Accurate detector alignment and excellent knowledge of the magnetic field are essential ingredients for precise measurements of the track parameters, and to achieve a precision on the absolute inner-detector momentum scale of better than 0.1%. The latter is needed for instance for a precise measurement of the W-boson mass at the LHC [5]. A campaign to measure the solenoid field map in the inner-detector cavity was undertaken in 2006, using a dedicated machine equipped with 150 Hall probes (reference [2], page 33). A total of more than 100000 points were measured, at five different magnet current values. As a result, a precision of about 4 Gauss (0.02%) was achieved on the knowledge of the magnetic field.

While waiting for collision data, the achieved knowledge of the detector alignment and of the magnetic field has been used to measure several performance aspects of the inner detector with cosmics data. This could be done, without resorting to simulation, by using the so-called “split-track" technique, i.e. by splitting cosmic muon tracks in the centre of the detector, refitting the two resulting tracks separately, and comparing their parameters. In this way it was possible to measure for instance the muon momentum resolution, shown in the left panel in figure 10: it is about 2% at a

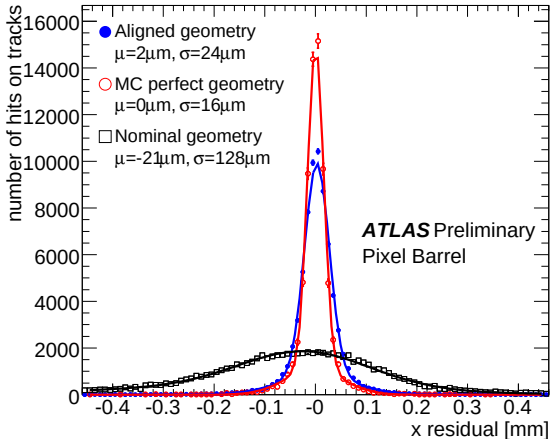

Figure 9: Distributions of the Pixel detector residuals, as obtained with cosmics data, before (open black squares) and after (closed blue points) alignment. The red open points show the distribution obtained from the Monte Carlo simulation for a perfectly aligned detector. The curves are fit to the points.

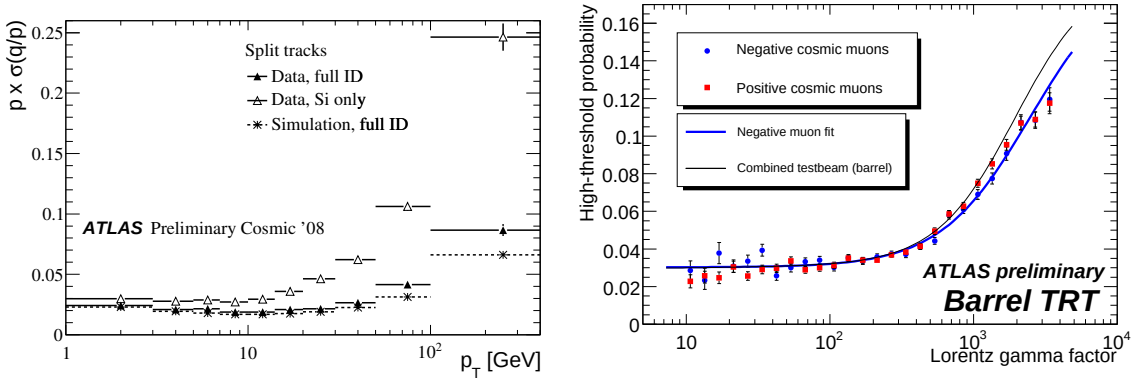

Figure 10: Left: Muon momentum resolution as a function of the muon transverse momentum, as measured in the inner detector with cosmics data using the Silicon layers only (open triangles) and the full inner detector (closed triangles). The stars show the simulation prediction for a perfectly aligned geometry. Right: Probability for emitting transition radiation in the TRT detector, as a function of the muon γ factor, as measured with cosmics data for negative-charge (blue dots) and positive-charge (red squares) muons. The thin black line shows the measurement previously obtained with test-beam data. The blue tick line is a fit to the negative cosmics muons.

few GeV, in the region where the precision is limited by multiple scattering in the detector material, and about 4% at 100 GeV. These results are well reproduced by the simulation, except at large momentum where residual misalignments in the data deteriorate the intrinsic detector resolution.

The Transition Radiation detector (TRT) is used for tracking (providing a factor $\sim$2 improvement in momentum resolution at $\sim$100 GeV, as shown in the left panel in figure 10, thanks to its large lever arm), as well as for particle identification. The latter is based on the fact that the intensity of the transition radiation emission is proportional to the particle Lorentz factor γ. The onset of transition radiation occurs for $\gamma \sim 1000$, as shown in the right panel in figure 10: as a consequence electrons emit transition radiation for momenta as low as $\sim$1 GeV, whereas muons and pions do so

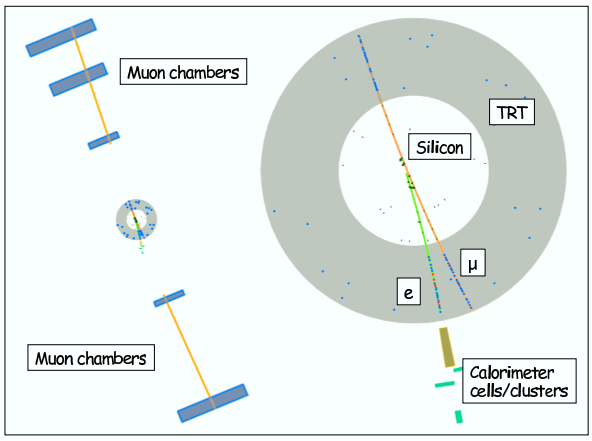

Figure 11: Sketched transverse view of the ATLAS detector showing a cosmics event recorded on 28 September 2008. The muon, coming from the top and traversing the full detector, produces a ionization electron in the Pixel detector.

only above $\sim$100 GeV.

The TRT information has been a crucial ingredient to observe an "electron signal" in the recorded cosmics data samples. These electrons are δ-rays (ionization electrons) produced by the primary cosmic muon. An example of such an event is shown in figure 11: the incident muon traverses the full detector, from top to bottom, and produces a high-energy δ-ray in the inner detector, which in turn gives rise to an energy deposition in the electromagnetic calorimeter.

To isolate an electron signal in the cosmics sample, events containing two reconstructed tracks were selected. One of the tracks was required to point to an energy deposition above 3 GeV in the electromagnetic calorimeter ("electron candidate"). For electron candidates in the selected two-track sample, the right panel in figure 12 shows the TRT energy deposition as a function of E/p, the ratio between the energy measured in the calorimeter and the track momentum measured in the inner detector. Electrons are expected to produce a large TRT signal and have $E/p \simeq 1$. Therefore, they populate mostly the central part of the plot (above the horizontal line and between the two vertical lines). In contrast, events with only one (muon) track emitting a hard Bremsstrahlung photon (shown for comparison in the left panel in figure 12) cluster mainly in the region of small TRT energy and small E/p. Finally figure 13 shows the E/p distribution for events with a large TRT signal (those above the horizontal line in figure 12) from the two-track sample. A clear "electron peak" is visible for $E/p \sim 1$. There are 36 electron candidates in the "signal" region between the two vertical lines, 32 of which have a negative charge, out of an initial sample of 3.5 million cosmics events. The estimated background is about 7 events.

Single-beam data recorded in September 2008 before the LHC incident provided complementary information to cosmics. The most useful events were obtained with a set-up where the tertiary collimators located at $\pm$140 m from the detector centre were closed, and the beam bunches (containing typically 2×10^9 protons, at a beam energy of 450 GeV) were smashed onto them. Such high-intensity interactions, called "beam splashes", produced an avalanche of secondary particles, depositing up to 3000 TeV in the calorimeters, and giving rise to thousands of tracks in the inner

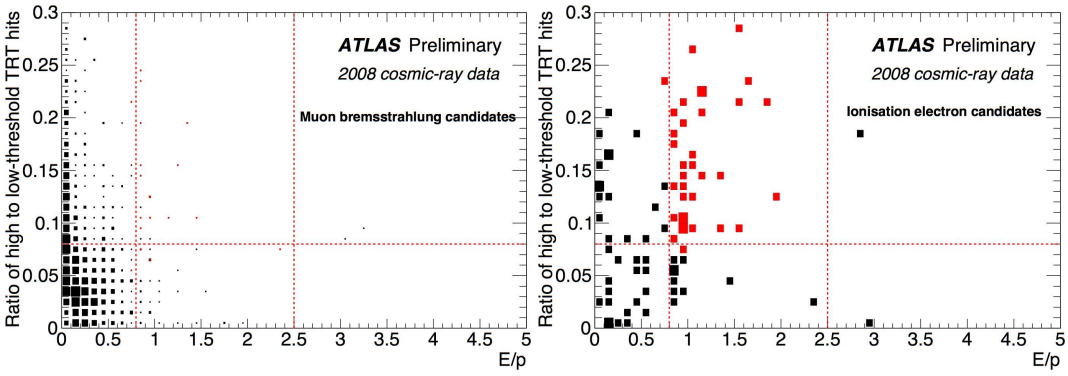

Figure 12: Fraction of transition-radiation hits in the TRT, as a function of the E/p ratio (see text), for cosmic muon events. Left: Events with one reconstructed track where the muon undergoes a hard Bremsstrahlung. Right: Events with two reconstructed tracks with an electron candidate (in this case only the latter is included in the plot). The red squares indicate tracks passing additional electron identification criteria.

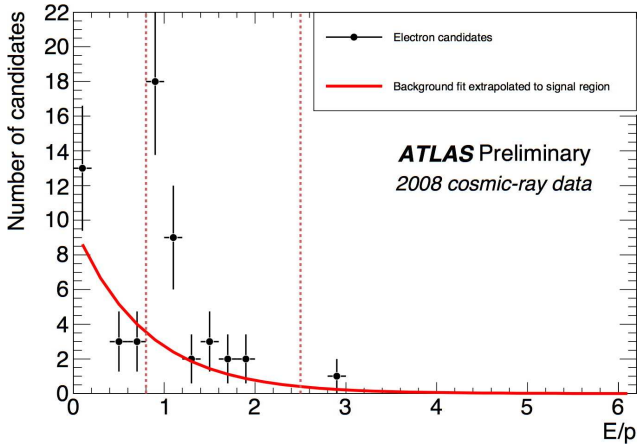

Figure 13: The E/p ratio for electron candidates in a sample of cosmics data containing two tracks (see text). The "signal" region is defined by the vertical dashed lines. The full line indicates the expected background, obtained by extrapolating from the one-track muon Bremsstrahlung sample.

detector and muon spectrometer.

These high-energy and high-track multiplicity beam-splash events have proved to be very useful to synchronize and cross-time the various trigger and detector components. This was done with respect to an absolute and stable time reference provided by dedicated devices (beam pickups, BPTX) located at $\pm$175 m from the detector centre, which detect the bunch passage with a time resolution of $\sim$50 ps. Figure 14 shows, for a sample of single-beam events triggered by the BPTX devices, the timing of some level-one trigger items (electromagnetic cluster, jet, tau, muon, etc.) with respect to the BPTX time, before (left panel) and after (right panel) timing adjustment. In only a couple of days, the timing spread of most of them was reduced from several bunch-crossings (one bunch-crossing corresponds to 25 ns) to one bunch-crossing.

In conclusion, cosmics and single-beam data have allowed an extensive commissioning of the detector, and remarkable improvements in the understanding of its performance. Further progress

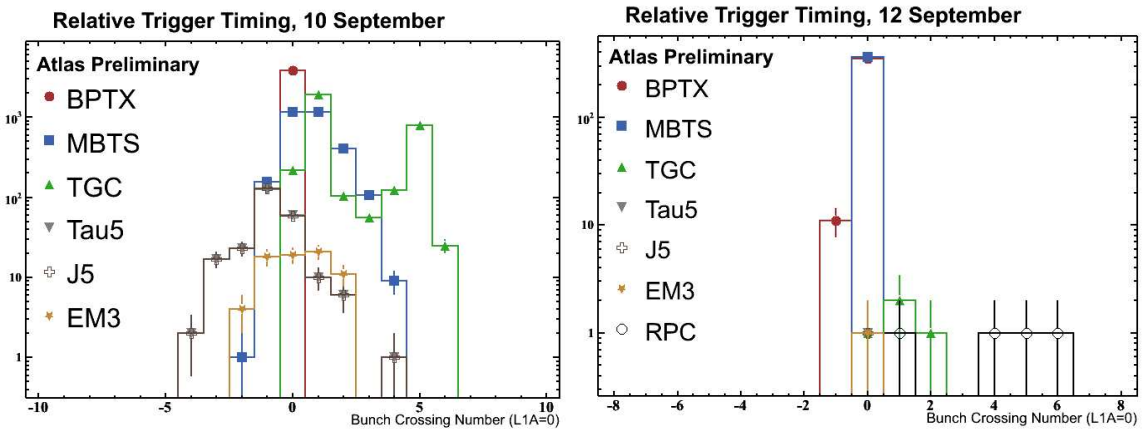

Figure 14: Timing distribution of some level-one triggers with respect to the reference provided by the BPTX devices, as obtained with single-beam data. The units of the x-axis are bunch-crossings (one bunch-crossing corresponds to 25 ns). Results are shown before (left) and after (right) time adjustment. The latter was applied to all triggers except the RPC muon trigger.

at this stage is only possible with collision data.

4. First physics with first data

With the advent of first collisions, two tasks need to be undertaken with the highest priority:

- Complete the commissioning and calibration of the detector and trigger beyond what could be achieved with cosmics and single-beam data, using well-known physics samples (such as leptonic Z-boson decays).
- "Re-discover" the Standard Model (SM) in the new energy domain offered by the LHC. Measurements of known processes, such as W, Z, top-quark, jet production, are not only important in their own right, but also because these channels are potential backgrounds to searches for new physics.

These two steps will take time, but are essential to prepare a solid road towards discoveries.

Figure 15 shows, for some representative processes, the expected number of events in ATLAS, as a function of the centre-of-mass energy, after simple selection cuts, for an integrated luminosity of 100 pb^{-1}. The latter should be collected by the end of 2010.

The size of the projected data samples depends on the exact centre-of-mass energy, expected to be between 7 and 10 TeV in the first LHC run. Typically, samples of about one million $J/\psi \to \mu\mu$ events should become available by the end of 2010, as well as few hundred thousands to one million W leptonic decays, and 50000-100000 $Z \to ee, \mu\mu$ events. Top-quark pairs should be routinely produced by the end of 2010, with 300-900 semi-leptonic $t\bar{t}$ final states expected per lepton species, depending on the centre-of-mass energy. Finally, if Supersymmetry exists, and squarks and gluinos have masses around 450 GeV (i.e. just above the reach of the Tevatron collider), 10-20 events could be recorded in 2010. These numbers indicate that, even with a modest amount of integrated

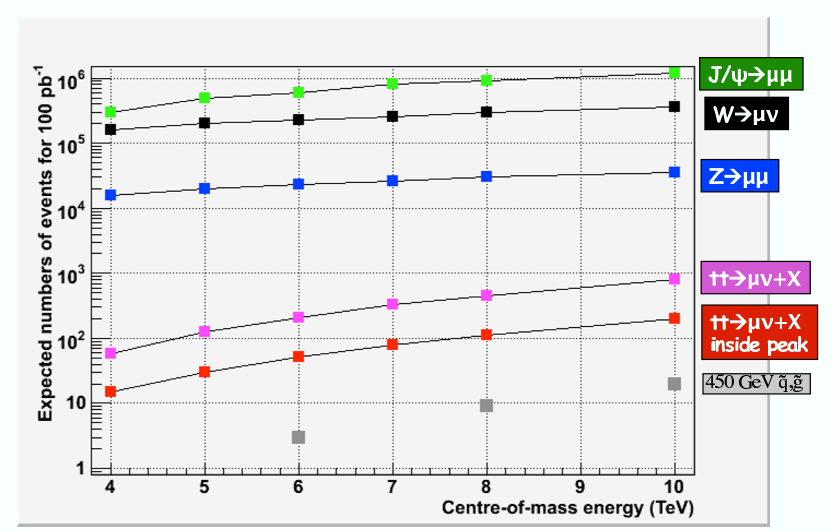

Figure 15: Expected number of events in ATLAS, as a function of the centre-of-mass energy, for several physics channels, after selection cuts and for an integrated luminosity of 100 pb^{-1}.

luminosity, the LHC will offer enough data for very useful detector performance studies, and for first exciting physics exploration.

The first step will be to observe well-known SM particles ($J/\psi, W, Z$, later on the top quark), so-called "standard candles". Such observations would provide a reassuring demonstration that the experiment works well, and would help refine the understanding and tuning of the detector performance.

In particular, $J/\psi, Y \rightarrow \mu\mu$ and $Z \rightarrow ee, \mu\mu$ (figure 16) are excellent tools to align the inner detector and muon spectrometer, to intercalibrate the electromagnetic calorimeter, to set the overall energy and momentum scale of the experiment, and to study lepton trigger, reconstruction and identification in detail. Typical expected precisions on these performance parameters are at the level of a few percent for integrated luminosities of 100-200 pb^{-1} [5].

A few ten of pb^{-1} should be enough to establish a top-quark signal, using for instance single-lepton final states ($t\bar{t} \rightarrow bWbW \rightarrow bjjb\ell\nu$). A simple analysis [6] would require one isolated lepton (electron or muon) with p_T >20 GeV, missing transverse energy (E_T^{miss}) in excess of 20 GeV, and at least four high-p_T jets, two of which having an invariant mass compatible with the W mass. No b-tagging of two of the jets would be required at the beginning, assuming (conservatively) that the performance of the vertex detector would not have been well understood at this early stage of the experiment. Figure 17 shows the expected signal in the electron channel on top of the background at $\sqrt{s} = 10$ TeV, for an integrated luminosity of 200 pb^{-1} (the signal yield is expected to be a factor ~ 2.5 smaller at $\sqrt{s} = 7$ TeV). Observation and measurements of top events mark at the same time an arrival and a starting point in the LHC physics roadmap. On one hand $t\bar{t}$ final states contain most physics objects (leptons, jets, b-quark jets, missing energy). Therefore the ability to measure these final states demonstrates that the detector performance, the calibration procedures and the reconstruction tools for the basic physics signatures are well understood and have achieved

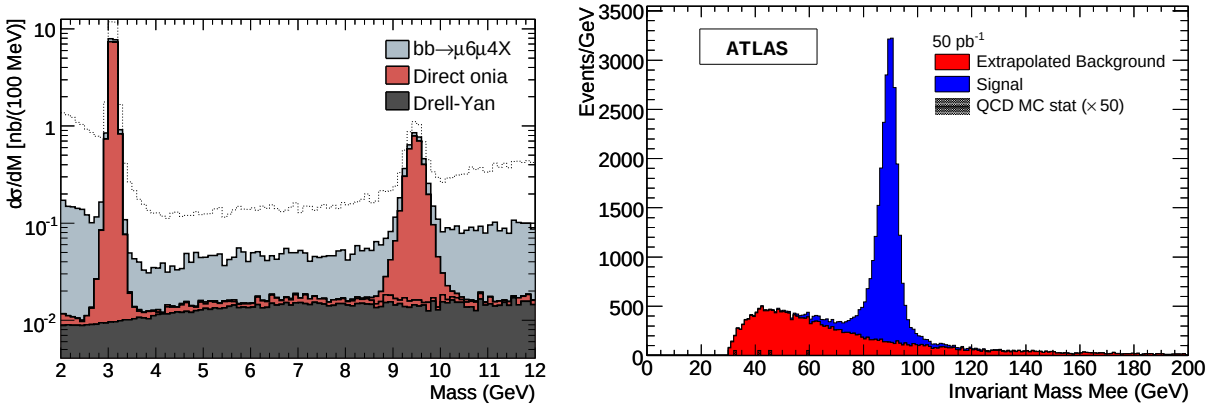

Figure 16: Left: The expected di-muon invariant mass cross-section for the $J/\psi \to \mu\mu$ and $Y \to \mu\mu$ signals and the backgrounds, after selection cuts, at $\sqrt{s} = 14$ TeV (the J/ψ yield after cuts is a factor ~2.5 smaller at $\sqrt{s} = 7$ TeV). The trigger requires two muons with $p_T > 6$ GeV and $p_T > 4$ GeV ($\mu 6\mu 4$). The dashed line indicates the background before requiring that the di-muon pair originates from the primary vertex. Right: The expected di-electron invariant mass distribution for the $Z \to ee$ signal (blue histogram) and the background (red histogram) after all selection cuts. The number of events corresponds to an integrated luminosity of 50 pb^{-1} at $\sqrt{s} = 14$ TeV (the expected $Z \to ee$ yield is ~40% smaller at $\sqrt{s} = 7$ TeV).

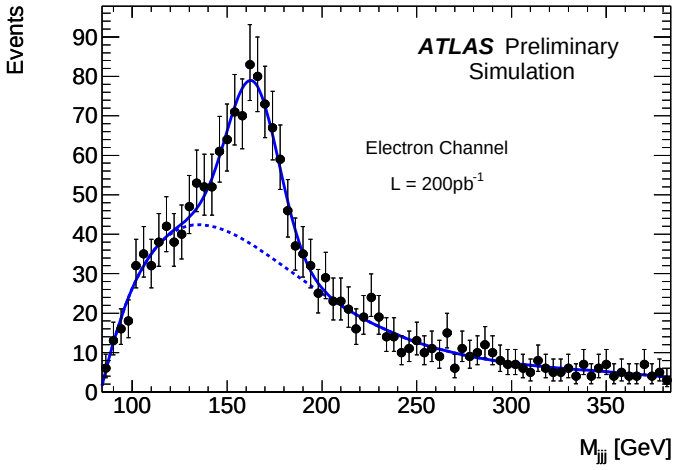

Figure 17: The expected three-jet invariant mass distribution for events selected as described in the text, showing the $t\bar{t} \to e+X$ signal on top of the background (dotted blue line). The number of events corresponds to an integrated luminosity of 200 pb^{-1} at $\sqrt{s} = 10$ TeV.

an excellent level of maturity. When this stage is achieved, the experiment's commissioning phase can be considered to be close to completion. On the other hand, $t\bar{t}$ production is one of the main backgrounds to most searches for new physics, and therefore top studies are the necessary first step in the path towards discoveries.

One of the most promising candidates for an early discovery is Supersymmetry (SUSY). Indeed, if SUSY has something to do with stabilizing the Higgs mass, new particles are expected at the TeV scale, and some of them (e.g. squarks and gluinos) could be discovered rather quickly.

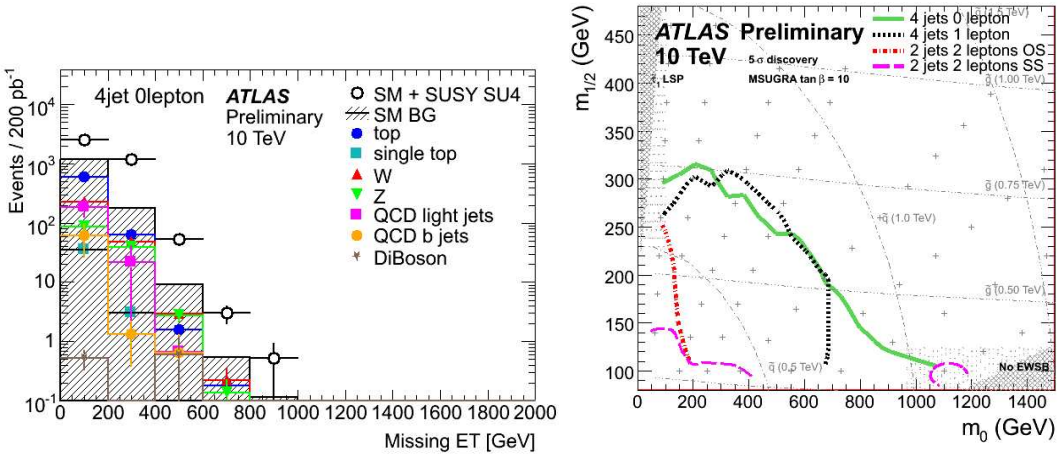

Figure 18: Left: The transverse energy spectrum expected in ATLAS for events with four high-p_T jets after all cuts, at $\sqrt{s}$ =10 TeV and for an integrated luminosity of 200 pb^{-1}. The open dots show the sum of the signal due to the production of $m \sim$400 GeV $\tilde{q}$ and $\tilde{g}$ and the SM background; the full histogram shows the total background and the closed symbols the various background contributions. Right: The expected 5σ discovery reach (the regions below the various curves) in ATLAS over the mSUGRA $m_0 - m_{1/2}$ plane for $\sqrt{s}$=10 TeV, an integrated luminosity of 200 pb^{-1}, and various final-state signatures. Lines of constant $\tilde{q}$ and $\tilde{g}$ masses are shown.

This is because of the huge production cross-section for squarks and gluinos, which are strongly-interacting particles, at high-energy hadron colliders. About two events per week are expected to be produced in ATLAS at $\sqrt{s}$=10 TeV and an (initial) instantaneous luminosity of 10^{31} cm^{-2} s^{-1} for $\tilde{q}$ and $\tilde{g}$ masses as large as $\sim$1 TeV. In addition, cascade decays of (heavy) squarks and gluinos should give rise to clear-signature final states, containing several high-p_T jets, sometimes leptons and, in R-parity conserving models, large missing transverse energy coming from the fact that the lightest neutralinos produced at the end of the decay chains escape detection.

The left panel in Figure 18 shows the missing transverse energy spectrum expected in ATLAS for events containing four high-p_T jets and large E_T^{miss} if squarks and gluinos exist and have a mass of about 400 GeV (corresponding to the Tevatron approximate reach). The signal is a factor of two larger than the SM background, but signal and background have a similar shape for these relatively light SUSY masses. Final states containing at least one high-p_T lepton, although less copious, provide a more convincing discrimination between signal and background, and are less sensitive to backgrounds coming from instrumental effects due to detector imperfections. They could therefore offer additional evidence for a genuine signal.

By using searches of this kind [7], ATLAS should be able to discover squarks and gluinos up to masses of $\sim$750 GeV at $\sqrt{s} \sim$10 TeV and for integrated luminosities as low as 200 pb^{-1}, as shown in the right panel in figure 18. For this small integrated luminosity, the discovery sensitivity should exceed the Tevatron exclusion reach ($m \sim$ 400 GeV), as long as the LHC centre-of-mass energy is larger than $\sim$7 TeV.

These goals can only be achieved if the tricky backgrounds, in particular fake missing transverse energy coming from instrumental effects (cracks in the detector, calorimeter response non-

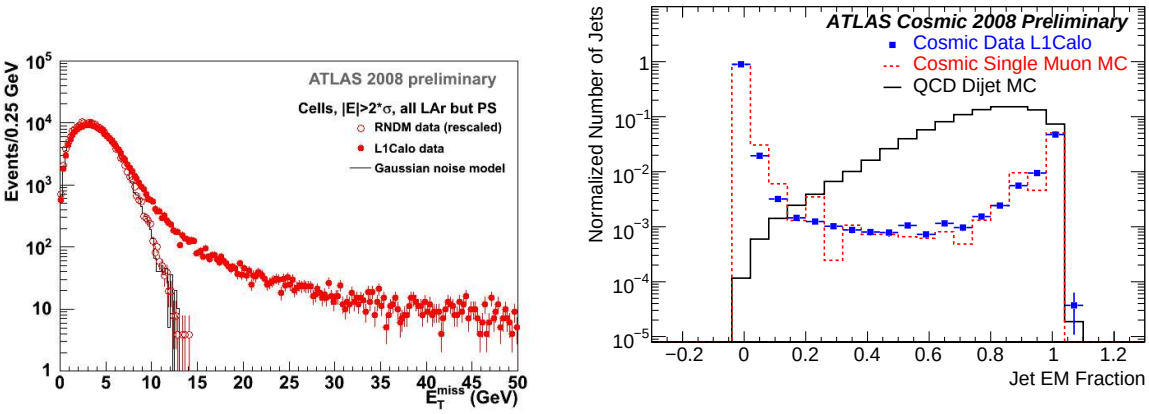

Figure 19: Left: The E_T^{miss} spectrum reconstructed in the liquid-argon calorimeters for cosmics events (closed dots) and for random triggers (open circles). Only calorimeter cells with energy $|E| > 2\sigma$ (where σ is the width of the cell noise distribution) are included in the E_T^{miss} calculation. The full line is the expectation from a Gaussian noise model. Right: The fraction of the jet energy deposited in the electromagnetic calorimeter for "jets" due to cosmic muon showers in the data (dots) and the cosmics Monte Carlo simulation (dashed red line), and for true jets from simulated QCD di-jet events (full black line). All distributions are normalized to the total number of jets in their respective samples.

linearities, noise, etc.), are well understood. This will take time. While waiting for collisions, some preliminary checks and studies could be made with cosmics data. The left panel in figure 19 shows the missing transverse energy distribution due to the calorimeter noise, as measured with randomly triggered events (empty events without genuine energy signals, triggered randomly by a dedicated clock). It can be deduced that the E_T^{miss} contribution from the electronic noise is small, and in agreement with the expectation. In particular, no significant sources of coherent noise have been observed. Another non-physical background to SUSY searches can potentially arise from a cosmics muon overlapping accidentally with a high-p_T proton-proton collision, for instance a di-jet event. Such an occurrence could produce an apparent missing transverse energy in an event that is a priori balanced. Rejection criteria to suppress these topologies have been preliminarily developed using the recorded cosmics data. The right panel in figure 19 shows that the fraction of energy deposited in the electromagnetic calorimeter by "jets" produced by cosmics muons is well reproduced by the simulation, and is very different from the fraction expected from genuine QCD jets. Shape variables of this type, combined with other criteria such as timing and vertex constraints, can be used to reject effectively the cosmics background to SUSY searches.

More examples of the ATLAS physics potential can be found in reference [5].

5. Conclusions

In July 2009, a few months before the LHC start-up, the ATLAS experiment is in excellent shape, from detector and trigger operation, to data quality, calibration and alignment, event simulation and reconstruction, data processing and worldwide distribution.

Over the last year, about 600 million cosmics events, as well as single-beam data, have been recorded successfully with the full detector operational. These data demonstrate a much better

detector performance than normally expected at this (early) stage of the experiment. In particular, calibration and alignment precisions good enough for first LHC physics studies have already been achieved. The software and computing infrastructure have proved to be able to cope with massive simulations, as well as real data from the detector, and with the complexity of a worldwide distributed system.

The exciting LHC physics programme, demonstrated over the years by increasingly realistic simulations, and now imminent, will reward 20 years of efforts of the international community to build an experiment of unprecedented technology, complexity and performance.

References

[1] L. Evans and P. Bryant editors, *LHC Machine*, *JINST* **3** (S08001) 2008.

[2] The ATLAS Collaboration, *The ATLAS Experiment at the CERN Large Hadron Collider*, *JINST* **3** (S08003) 2008.

[3] L. Evans, these Proceedings.

[4] I. Bird, B. Jones and K.F. Kee, *The organization and management of Grid infrastructures*, *IEEE Computer*, **42** (36) January 2009.

[5] The ATLAS Collaboration, *Expected performance of the ATLAS experiment: detector, trigger and, physics*, *CERN-OPEN-2008-020*.

[6] The ATLAS Collaboration, *Prospects for the top-pair production cross-section at* $\sqrt{s}$*=10 TeV in the single-lepton channel in ATLAS*, ATLAS Note *ATL-PHYS-PUB-2009-087*.

[7] The ATLAS Collaboration, *Prospects for Supersymmetry and Universal Extra-dimensions discovery based on inclusive searches at a 10 TeV centre-of-mass energy with the ATLAS detector*, ATLAS Note *ATL-PHYS-PUB-2009-084*.